HHS Public Access

Author manuscript

J Neuropathol Exp Neurol. Author manuscript; available in PMC 2015 November 01.

Published in final edited form as:

J Neuropathol Exp Neurol. 2014 November ; 73(11): 1078–1090. doi:10.1097/NEN.0000000000000126.

Combinatorial Therapy with Tamoxifen And Trifluoperazine Effectively Inhibits Malignant Peripheral Nerve Sheath Tumor Growth by Targeting Complementary Signaling Cascades

Stephanie N. Brosius, PhD[1,3,*], **Amy N. Turk, BS**[1,*], **Stephanie J. Byer, BS**[1], **Jody Fromm Longo, PhD**[4], **John C. Kappes, PhD**[2], **Kevin A. Roth, MD, PhD**[1], and **Steven L. Carroll, MD, PhD**[1,4]

[1]Department of Pathology, University of Alabama at Birmingham, Birmingham, Alabama

[2]Department of Medicine, University of Alabama at Birmingham, Birmingham, Alabama

[3]Medical Scientist Training Program, University of Alabama at Birmingham, Birmingham, Alabama

[4]Department of Pathology and Laboratory Medicine, Medical University of South Carolina, Charleston, South Carolina

Abstract

Chemotherapeutic agents effective against malignant peripheral nerve sheath tumors (MPNSTs) are urgently needed. We recently found that tamoxifen potently impedes xenograft growth. In vitro, tamoxifen inhibits MPNST proliferation and survival in an estrogen receptor-independent manner; these effects are phenocopied by the calmodulin inhibitor trifluoperazine. The present study was performed to establish the mechanism of action of tamoxifen in vivo and optimize its therapeutic effectiveness. To determine if tamoxifen has estrogen receptor-dependent effects in vivo, we grafted MPNST cells in castrated and ovariectomized mice; xenograft growth was unaffected by reductions in sex hormones. To establish whether tamoxifen and trifluoperazine additively or synergistically impede MPNST growth, mice xenografted with NF1-associated or sporadic MPNST cells were treated with tamoxifen, trifluoperazine, or both drugs for 30 days. Both monotherapies inhibited graft growth by 50%, whereas combinatorial treatment maximally reduced graft mass by 90% and enhanced decreases in proliferation and survival. Kinomic analyses showed that tamoxifen and trifluoperazine have both shared and distinct targets in MPNSTs. Additionally, trifluoperazine prevented tamoxifen-induced increases in serum/glucocorticoid regulated kinase 1, a protein linked to tamoxifen resistance. These findings suggest that combinatorial therapy with tamoxifen and trifluoperazine is effective against MPNSTs because these agents target complementary pathways that are essential for MPNST pathogenesis.

Send correspondence and reprint requests to: Steven L. Carroll, MD, PhD, Professor and Chair, Department of Pathology and Laboratory Medicine, Medical University of South Carolina, 171 Ashley Avenue, MSC 908, Charleston, SC 29425-9080. Phone: (843) 792-3121; Fax: (843) 792-0555. carrolst@musc.edu.

*These authors contributed equally to this manuscript.

The authors have no conflicts to declare.

Keywords

Kinomics; Neurofibromatosis; Peripheral nervous system; Preclinical study; Sarcoma; Schwann cell; Tamoxifen; Trifluoperazine

INTRODUCTION

Malignant peripheral nerve sheath tumors (MPNSTs) are aggressive peripheral nervous system neoplasms that arise from the Schwann cell lineage. These neoplasms are common in patients with the autosomal dominant tumor predisposition syndrome neurofibromatosis type 1 (NF1); the estimated lifetime risk of developing an MPNST in these patients is 8% to 13% (1). MPNSTs arise via progression from benign tumors of large nerve plexuses known as plexiform neurofibromas in NF1 patients (1, 2); however, they may also occur sporadically in the general population where they typically arise de novo. Overall, about half of all MPNSTs present in NF1 patients, with the remainder occurring sporadically.

Both sporadic and NF1-associated MPNSTs have a poor prognosis; 5- and 10-year survival rates for patients with these neoplasms are 34% and 23%, respectively (3, 4). In large part this is because there are no effective chemotherapeutic regimens for MPNSTs and because radiotherapy does not extend the survival of these patients. At present, surgery is the only effective means of treating MPNSTs but the effectiveness of surgery is frequently limited by the fact that MPNSTs aggressively invade local tissue and metastasize widely. Consequently, the development of new chemotherapeutic regimens that effectively target MPNSTs is essential if we are to improve the prognosis of patients with these high-grade tumors.

Although controversial, some previous reports have argued that sex steroid hormones promote the pathogenesis and growth of human MPNSTs (5). In keeping with this possibility, we have found that MPNSTs express estrogen receptor-β (ERβ), the G-protein coupled estrogen receptor-1 (GPER), and both of the rate-limiting enzymes in the 2 major estrogen biosynthetic pathways (6). These observations led us to challenge human MPNST cells with 4-hydroxytamoxifen, an active metabolite of the selective estrogen receptor modulator tamoxifen. We found that 10- to 100-nM concentrations of this agent inhibited the proliferation of human MPNST cells in vitro, whereas 1- to 5-μM concentrations of tamoxifen induced MPNST cell death. Further, when we implanted pellets containing 25 mg of tamoxifen into mice orthotopically xenografted with MPNST cells, we found that the grafts were 50% smaller in tamoxifen-treated mice compared to animals receiving placebo tablets. Surprisingly, however, we also found that tamoxifen acts in an ER-independent manner in cultured MPNST cells and that it does so via multiple mechanisms. For instance, we established that the effects of tamoxifen on cultured MPNST cells were phenocopied by the calmodulin inhibitor trifluoperazine (6), suggesting that tamoxifen acts on MPNST cells at least in part by inhibiting calmodulin. We also showed that tamoxifen induces autophagic death in cultured MPNST cells by selectively degrading K-Ras (7). Nonetheless, our previous studies did not rule out the possibility that the effects of tamoxifen in vivo might reflect, in part, its action on estrogen receptors. This distinction is important because it raises

the question of whether reducing sex steroid levels would enhance the therapeutic effects of tamoxifen in patients with MPNSTs.

The goals of this study were to establish the optimal conditions for tamoxifen therapy of MPNSTs in vivo, to compare the effectiveness of tamoxifen and trifluoperazine monotherapy directly, and to determine whether combinatorial therapy with tamoxifen and trifluoperazine was superior to treatment with either agent alone. As the mechanisms of action of tamoxifen and trifluoperazine in MPNST cells remain incompletely understood, we also globally examined the effects that these agents exert on the tyrosine and serine/threonine kinases expressed in MPNST cells (i.e. the kinome) and then compared the actions that tamoxifen and trifluoperazine have on these kinases with an eye towards providing a mechanistic underpinning for combinatorial therapy with tamoxifen and trifluoperazine.

MATERIALS AND METHODS

Antibodies and Other Reagents

A mouse monoclonal antibody recognizing phosphorylated tyrosine residues (PY20; catalog #sc508) was obtained from Santa Cruz Biotechnology (Santa Cruz, CA). A mouse monoclonal anti-Ki67 antibody (#558078) was purchased from BD Biosciences (Franklin Lakes, NJ). Rabbit monoclonal antibodies recognizing serum/glucocorticoid-regulated kinase (SGK), phospho-SGK1 (D36D111), Akt, and phospho-Akt were purchased from Cell Signaling Technology (Danvers, MA). Secondary antibodies were from Jackson Immunoresearch, Inc. (West Grove, PA) and BD Biosciences (San Jose, CA). The Apoptag Peroxidase In Situ Apoptosis Detection Kit was purchased from Millipore (Billerica, MA).

4-Hydroxy-tamoxifen was obtained from EMD Chemicals (Gibbstown, NJ). Trifluoperazine dihydrochloride (#T8516) was purchased from Sigma-Aldrich (St. Louis, MO). Tamoxifen free base in pellet form (#E-361) was from Innovative Research of America (Toledo, OH) and in powder form (#T5648) was from Sigma-Aldrich.

Cell Lines and Culture

We previously described the sources of the human MPNST lines used in this study (6, 8, 9). ST88-14 and STS-26T cells were maintained in Dulbecco's modification of Eagle’s medium (DMEM) supplemented with 10% fetal calf serum, 10 μg/mL streptomycin and 10 IU/mL penicillin (DMEM10). Cell morphology and doubling times were examined regularly and all cells were tested via PCR analysis for mycoplasma at regular intervals (10). Cell identities were validated regularly via small tandem repeat analyses of 15 markers standardly utilized by the American Type Culture Collection and the amelogenin locus (to verify the sex of the patient from which the lines were derived) using an Applied Biosystems (Foster City, CA) AmpFISTR system.

Gonadectomies

Castration and ovariectomy surgeries were performed as previously described (11, 12). NOD.Cg-*Prkdc*^{scid}*Il2rg*^{tmlWjl}/SzJ mice (NSG mice; Jackson Laboratory stock #005557) (n = 32) underwent gonad removal or sham surgery. Animals were allowed to recover for 1

month prior to grafting to allow circulating sex hormones to reach trough levels (13, 14). ST88-14 cells were then grafted into the sciatic nerves of these mice, as described below. After 1 month, the mice were killed and their tumors removed and weighed. Statistical analysis was performed using the Student t-test; $p < 0.05$ was considered significant.

Orthotopic Xenografting and Stratification of Grafted Mice for Drug Trials

We previously described the production of ST88-14 cells stably transduced with a lentiviral vector in which the cytomegalovirus immediate early promoter drives expression of a firefly luciferase-internal ribosomal entry site (IRES)-puromycin resistance cassette (6). STS-26T cultures were transduced with the same lentiviral vector and then selected in DMEM10 containing 5 μg/mL puromycin. Expression was verified with bioluminescent imaging.

Orthotopic xenografting was performed using our previously described methodology (15). Briefly, 5×10^5 STS-26T or 5×10^3 ST88-14 cells were suspended in 5 μL or 3 μL DMEM10, respectively, and injected into the sciatic nerves of NSG mice. The number of cells injected was chosen based on preliminary experiments in which we empirically determined the minimum number of cells required to generate a tumor approximately 1 cm in diameter within 30 days. At 1 and 3 days post-grafting, bioluminescence imaging was performed using a Xenogen IVIS-100 system (Calipers Life Sciences, Hopkinton, MA) to verify graft establishment and to stratify mice into therapeutic cohorts, as previously described (15).

Tamoxifen and Trifluoperazine Treatment

Therapeutic regimens were begun at 3 days post-xenografting. Tamoxifen free base was administered either by subcutaneously implanted pellet or intraperitoneal injection in a peanut oil/ethanol suspension. To generate the suspension, tamoxifen free base was dissolved in 100% ethanol in a 55°C dry bath, diluted 1:10 in sterile peanut oil and vortexed. Trifluoperazine was dissolved in sterile phosphate buffered saline and administered intraperitoneally. Drugs were injected on a 5-day on/2-day off schedule for 30 days. Grafts were collected, weighed, and fixed in fresh 4% paraformaldehyde in phosphate buffered saline.

Determination of Ki67 Labeling and Terminal Deoxynucleotidyl Transferase dUTP Nick End Labeling Indices

FOUR-μm-thick Paraffin sections were used for all histology. Ki67 immunohistochemistry was performed per our previously described protocol (8). Terminal deoxynucleotidyl transferase dUTP nick end labeling (TUNEL) was performed using the Apoptag Peroxidase In Situ Apoptosis Detection Kit (Millipore) per the manufacturer's recommendations. Ki67 and TUNEL labeling indices were determined following our previously described methodology (6). Labeling indices were averaged and statistical comparisons performed using a one-way ANOVA with a Newman-Keuls Multiple Comparison test.

Kinomics

To establish the optimal time and drug concentrations for kinomic analyses, ST88-14 MPNST cells were treated with vehicle, 4-hydroxy-tamoxifen (2 or 4μM) or trifluoperazine

(2.5 or 5μM) for 5, 10, 15, 30, 60 and 120 minutes. Lysates were prepared in Mammalian Protein Extraction Reagent (MPER, Thermo Scientific; Rockford, IL) per the manufacturer's recommendations, immunoblotted per our previously described methodology (16) and probed with PY20 antibody (1:200 dilution) to determine the times at which tyrosine phosphorylation was maximally inhibited. Equivalent loading was verified by reprobing membranes with an anti-glyceraldehyde 3-phosphate dehydrogenase antibody (1:20,000 dilution).

Kinomics analyses were performed using a PamStation 12 automated kinomics instrument with phosphotyrosine and phosphoserine/phosphothreonine arrays (PamGene; Hertogenbosch, The Netherlands). ST88-14 cells were treated with vehicle, 2 μM 4-hydroxy-tamoxifen or 5 μM trifluoperazine for 10 or 30 minutes, respectively, and then lysed in MPER. Lysates were filtered through a 0.2-μm filter and diluted to 1 mg/mL. Ten μg of lysate was applied to PamChip 4 arrays in 1xABL buffer (New England Biolabs, Ipswich, MA) containing 100 μM ATP and 5 μg/mL FITC-conjugated anti-phosphotyrosine or anti-phosphoserine/phosphothreonine antibodies. The assay mix was pumped onto the wells and a first exposure was read. A kinetic reading program was run for 40 minutes, with readings taken every 5 minutes via CCD camera. Three technical replicates were run per condition. Spot images were quantified and linked to peptide identities with Bionavigator software (PamGene). Data were fit to a curve using CurveFitHT software (PamGene) with the Vinip2 curve-fitting algorithm applied over the first 30 minutes of the assay. Initial velocities were derived at the first kinetic time point read. Data from visually damaged wells or wells with inter-replicate correlation coefficients <0.95 were excluded. Peptides with paired t-test $p < 0.05$ values were considered significantly altered. These peptides were utilized to generate a list of probable upstream kinases phosphorylating these sites via the Kinexus Phosphonet platform (www.phosphonet.ca).

Immunoblot Analyses

Cells were homogenized in HES buffer (40 mM HEPES, 2 mM EDTA, 500 mM sucrose) supplemented with protease (Sigma-Aldrich #P8340) and HALT phosphatase (Thermo Scientific #78420) inhibitor cocktails (1:100 dilution). A modified Lowry method was used to determine protein concentrations (DC Protein Assay; Bio-Rad, Hercules, CA). Protein lysates were resolved on 8% SDS-polyacrylamide gels, immunoblotted per our previously described methodology (16), and probed with antibodies recognizing SGK1, phospho-SGK1, Akt or phospho-Akt (all at a 1:1000 dilution). Immunoreactive proteins were detected using enhanced chemiluminescence (Thermo Scientific).

RESULTS

Gonadally Derived Sex Steroids Do Not Enhance Xenograft Growth

We have shown that tamoxifen inhibits the proliferation and survival of cultured MPNST cells in an estrogen receptor-independent fashion (6). However, other investigators have presented evidence that estrogen can enhance MPNST growth (18). Consequently, we were reluctant to rule out the possibility that estrogen might promote MPNST growth in the more complex in vivo environment. We postulated that reducing circulating sex hormone levels

would impair the growth of orthotopically xenografted MPNST cells if sex hormones promote MPNST growth in vivo; further, should this postulate prove to be correct, the effectiveness of tamoxifen treatment might be enhanced by castration or ovariectomy. We therefore performed castration, ovariectomy, or sham surgeries on 18 male and 14 female NSG mice. Animals were allowed to recover for 1 month, a period that is sufficient for gonadally derived sex hormones to reach trough levels in the circulation after gonadectomy (13, 14). Gonadectomized and sham operated mice were then orthotopically xenografted with ST88-14 MPNST cells and the grafts were allowed to grow for 1 month. At the end of this time, tumors were harvested and weighed. We found that neither ovariectomy (Fig. 1A), nor castration (Fig. 1B), significantly altered graft weight compared to the tumors in sham-operated animals. We conclude that diminishing the levels of circulating sex hormones does not affect the growth of orthotopically xenografted human MPNST cells. Based on these observations, it is thus unlikely that the effectiveness of tamoxifen would be further enhanced by ovariectomy or castration.

Establishing the Maximal Inhibitory Effect of Tamoxifen on MPNST Xenografts

In our earlier study, we orthotopically xenografted MPNST cells in NSG mice and demonstrated that the grafts in animals surgically implanted with tamoxifen pellets (25 mg of tamoxifen in a matrix that released the drug continuously over 60 days) were 50% smaller than grafts in control mice receiving placebo pellets (6). While these encouraging observations indicated that tamoxifen inhibits MPNST xenograft growth, it was not clear that the concentration of tamoxifen we used in that study was sufficient to achieve the maximal inhibitory effect of tamoxifen on MPNST graft growth. Consequently, we examined the effect that different concentrations of tamoxifen exerted on the growth of orthotopically xenografted MPNST cells.

For these experiments, the sciatic nerves of 80 male NSG mice were surgically exposed and orthotopically xenografted with 5×10^3 luciferase-tagged ST88-14 MPNST cells. At 3 days post-grafting, these mice were divided into 4 equally sized cohorts (20 mice per group). Each animal was subcutaneously implanted with pellets containing placebo or 5, 25 or 50 mg of tamoxifen free base; these pellets were formulated to release a constant amount of drug for 60 days. Mice were then examined weekly with bioluminescence imaging so that tumor responses to treatment could be assessed in vivo. Quantification of the bioluminescent signals from the xenografts showed that luminosity was similarly diminished out to 30 days post-grafting in mice implanted with 25 and 50 mg tamoxifen pellets (Fig. 2A) compared to animals receiving the placebo pellets. In contrast, the bioluminescent signals in grafted mice implanted with 5 mg tamoxifen pellets were not significantly different from that seen in grafted animals carrying placebo pellets. In keeping with this, we found that the weights of grafts removed from mice implanted with 25 mg and 50 mg tamoxifen pellets were significantly decreased in comparison to grafts from animals receiving placebo (Fig. 2B), whereas the weights of the 5 mg tamoxifen and placebo treated grafts were similar. Notably, however, there was no significant difference in graft weight between the 25 mg and 50 mg treatments. We conclude that the 25 mg tamoxifen pellets are sufficient to maximally inhibit graft growth.

Trifluoperazine Monotherapy Inhibits the Growth of Xenografted MPNST Cells

We have previously shown that trifluoperazine, a drug the mechanism of action of which partially overlaps with that of tamoxifen, also inhibits the proliferation and survival of cultured human MPNST cells. However, we did not determine whether trifluoperazine effectively inhibits the growth of MPNST grafts in vivo and, if so, how the effectiveness of trifluoperazine compares to that of tamoxifen. Consequently, we next performed a direct comparison of the ability of tamoxifen and trifluoperazine to inhibit the growth of MPNST xenografts. Because trifluoperazine pellets analogous to the tamoxifen pellets described above were not available, performing this experiment required that we first develop an intraperitoneal injection regimen for delivering both drugs. We began by determining the maximum tolerated dose (MTD) of tamoxifen and trifluoperazine administered via intraperitoneal injection. For this purpose, groups of three mice were treated with each agent for 1 month, following a dosing regimen in which animals received 5 consecutive days of intraperitoneally injected drug, with 2 days rest in between. This dose was increased until adverse effects such as weight loss, alterations in grooming behavior, or death were observed (a “3+3” regimen). Using this approach, we established the MTD of tamoxifen in NSG mice as 30 mg/kg, while the MTD of trifluoperazine was 20 mg/kg.

We next compared the effectiveness of trifluoperazine and tamoxifen at their MTD. For these experiments, we orthotopically xenografted 24 male NSG mice with ST88-14 cells. As before, bioluminescent imaging was performed 3 days post-grafting to verify that the grafts had established. The grafted mice were then divided into 3 cohorts, each of which received intraperitoneal vehicle, 30 mg/kg tamoxifen or 20 mg/kg trifluoperazine dihydrochloride for a total of 30 days following the regimen described above. At the end of this period, tumors were harvested and weighed. As shown in Figure 3A the xenografts from tamoxifen-treated mice were approximately 50% smaller than those from vehicle controls. This reduction in xenograft size in mice receiving tamoxifen via intraperitoneal injection was thus highly similar to that seen in mice implanted with 25 or 50 mg tamoxifen pellets (Fig. 2B), indicating that our intraperitoneal injection regimen had an effect on graft growth analogous to the maximal effect seen with implanted tamoxifen pellets. The sizes of the MPNST xenografts in trifluoperazine-treated mice were also significantly reduced, being approximately 40% smaller than the grafts collected from mice receiving vehicle (0.49 grams vs. 0.31 grams, $p < 0.05$) (Fig. 3B). We conclude that tamoxifen and trifluoperazine both effectively inhibit MPNST xenograft growth when administered at their MTD, with the maximal effect produced by tamoxifen and trifluoperazine administered as single agents being an inhibition of graft growth in the range of 40% to 50%.

Combined Tamoxifen and Trifluoperazine Therapy More Effectively Inhibits Graft Growth than Either Agent Alone

Previous studies indicated that some proteins (e.g. calmodulin) are targeted by both tamoxifen and trifluoperazine, while others are targeted by only one of these drugs. The possibility that tamoxifen and trifluoperazine might target distinct molecules in MPNSTs raised the question of whether treatment with both agents would be more effective than treatment with either agent alone. To test this, we grafted ST88-14 cells into male NSG mice and treated them for 30 days with vehicle, tamoxifen alone, trifluoperazine alone, or both

drugs, using dosages slightly below the MTD for tamoxifen (25 mg/kg) and trifluoperazine (15 mg/kg). This study was repeated in 3 independent cohorts of mice. Aggregate data for all 75 animals are shown in Figure 4A. Monotherapy with either tamoxifen or trifluoperazine reduced tumor size by approximately 40% ($p < 0.0001$), whereas combined treatment with both drugs produced a reduction of 73.6% ($p < 0.01$). To determine if combinatorial treatment also inhibited the proliferation and survival of xenografted MPNST cells to a greater extent than tamoxifen or trifluoperazine alone, we performed Ki67 and TUNEL staining on 5 tumors from each treatment group (Fig. 5A-D) and quantified the Ki67 and TUNEL labeling indices in these grafts (Fig. 5E-H). We found that tamoxifen decreased proliferation by 3.9% compared to vehicle controls, whereas trifluoperazine decreased proliferation by 7.3% and combinatorial treatment decreased the Ki67 labeling index by 12.5% ($p < 0.01$, Fig. 6A). Combined treatment also significantly increased TUNEL indices within the grafts compared to grafts receiving tamoxifen or trifluoperazine alone ($p < 0.001$; Fig. 6B). In contrast, although Ki67 and TUNEL labeling was significantly altered in grafts treated with tamoxifen or trifluoperazine alone compared to vehicle controls, there was no significant difference in the Ki67 and TUNEL labeling indices when tamoxifen or trifluoperazine treated grafts were compared to one another.

We next repeated this study in 48 mice using the sporadic STS-26T MPNST cell line. To ensure that there was no sex effect on responsiveness to tamoxifen or tamoxifen-trifluoperazine therapy, we included both male and female mice in these cohorts. As was seen with ST88-14 cells, STS-26T cells demonstrated a significant difference in graft size when comparing tamoxifen only and trifluoperazine only-treated grafts to vehicle controls ($p < 0.0001$; Fig. 4B). Combined therapy again additively inhibited graft growth, producing an 87% reduction in tumor weight when compared to vehicle, whereas monotherapy with tamoxifen or trifluoperazine produced a maximum inhibition of approximately 50%. We saw no significant differences between the tumor weights in male and female mice in any of these cohorts. When analyzing Ki67 labeling indices, we similarly observed an additive reduction in proliferation in tumors treated with both tamoxifen and trifluoperazine when compared to grafts receiving monotherapy or vehicle (Fig. 6C, $p < 0.0001$). Dual treatment also doubled TUNEL labeling within the grafts (Fig. 6D, $p < 0.001$). As in our studies using ST88-14 cells, no significant difference in Ki67 or TUNEL labeling was observed when grafts receiving tamoxifen or trifluoperazine were compared to one another. We conclude that combinatorial treatment of MPNSTs with tamoxifen and trifluoperazine inhibits tumor proliferation and survival to a greater extent than is seen when these grafts are treated with tamoxifen or trifluoperazine as individual therapies.

Tamoxifen and Trifluoperazine Act on Overlapping and Distinct Cellular Signaling Cascades in MPNST Cells

At present, virtually nothing is known regarding the signaling pathways affected by tamoxifen and trifluoperazine in MPNST cells. However, our demonstration that combinatorial therapy with tamoxifen and trifluoperazine is more effective than treatment with either agent alone suggest that these drugs differ in their effects on key signaling cascades. Consequently, we next attempted to identify the kinases the actions of which are

altered by tamoxifen and trifluoperazine in MPNST cells and to compare alterations in kinome activation in tamoxifen- and trifluoperazine-treated cells.

To identify the signaling cascades that are impacted by tamoxifen and trifluoperazine treatment, we performed kinomics analysis on ST88-14 cells treated with the IC_{50} concentration of tamoxifen or trifluoperazine for 10 or 30 minutes, respectively, in depleted media; depleted media was utilized to minimize alterations in kinase signaling induced by growth factors present in serum. These treatment times were selected because they represent the time points at which global phosphorylation was maximally inhibited as assessed by probing Western blots with an anti-phosphotyrosine antibody. To perform our kinomic analyses, we used the PamGene system, an instrument in which cellular lysates are applied to arrays of target peptides and the phosphorylation of these peptides is quantified throughout the incubation period of the assay. We used 2 types of arrays that carried target peptides for either serine/threonine kinases or tyrosine kinases so as to capture the broadest range of signaling changes; the serine/threonine kinase arrays contain 144 target peptides with over 200 phosphorylatable residues, whereas the tyrosine kinase arrays detect 140 phosphorylation sites on a total of 100 target peptides. Target peptides identified in this process were then analyzed using the Kinexus Phosphonet database, which utilizes an algorithm that identifies kinases most likely targeting the given phosphorylation site. Three technical replicates were performed for each sample.

As shown in the Table, treatment with trifluoperazine decreased the phosphorylation of numerous peptides relative to tamoxifen treatment. In keeping with our previous findings with tamoxifen and a potential overlap in tamoxifen and trifluoperazine action, trifluoperazine treatment resulted in decreases in the phosphorylation of Erk1/2, Akt, and JNK, demonstrating that tamoxifen and trifluoperazine target some of the same signaling cascades in MPNST cells. However, trifluoperazine treatment also altered the phosphorylation of several signaling molecules in comparison to tamoxifen treatment. Notably, these cytoplasmic signaling molecules included several proteins such as serum/glucocorticoid regulated kinase (SGK), PIM-1, PIM-3, and protein kinase A, which have been implicated in either the proliferation or survival of other tumor types or the proliferation of non-neoplastic Schwann cells. The results for selected targets such as Akt and SGK1 were validated via Western blot (Fig. 7A-C). To verify these results further, we also treated 2 additional MPNST cell lines (STS-26T cells and T265-2c cells, a line derived from an NF1-associated MPNST) with tamoxifen or trifluoperazine and examined the effects that these treatments had on SGK1 expression and phosphorylation and Akt phosphorylation. Although there were some differences in the timing of the changes in SGK1 expression and Akt phosphorylation, tamoxifen and trifluoperazine had effects on these kinases in both STS-26T and T265-2c cells that were analogous to those observed in ST88-14 cells (Supplemental Figs. 1, 2, respectively).

Among these proteins, SGK was of particular interest because this protein is a serine/threonine kinase that is both related to Akt and modulated by the same signaling cascades. Much like Akt, SGK1 activation promotes cell cycle progression and evasion of apoptosis, both of which enhance tumorigenesis (22-24). Further, in breast cancer, resistance to tamoxifen is largely mediated by increased signaling via the PI3K/Akt axis; elevated SGK1

levels correlate with tamoxifen resistance, which has led to the suggestion that SGK1 signaling is involved in this process (25). To validate our data further and examine tamoxifen and trifluoperazine effects on SGK1 in more detail, we next examined the expression and phosphorylation of SGK1 in ST88-14 human MPNST cells that had been treated with 2μ M tamoxifen or 5μ M trifluoperazine for times ranging from 10 minutes to 24 hours. In vehicle (DMSO)-treated cells, SGK1 was undetectable, whereas in ST88-14 cells treated with tamoxifen we saw a prominent increase in the expression of a protein of the expected 50 kDa size by 10 minutes after tamoxifen exposure (Fig. 7C, middle panel); this time course is consistent with previous reports in other tumor types where SGK1 has been shown to be rapidly upregulated within 30 minutes of exposure to a growth factor or another stimulus (26). Additionally, phosphorylation of SGK also increased with tamoxifen treatment in concordance with protein levels (Fig. 7C, top panel). This increase in SGK1 expression and phosphorylation was absent in trifluoperazine-treated cells (Fig. 7D).

Given the distinct effects of tamoxifen and trifluoperazine on SGK1 expression and phosphorylation and the potential role of SGK1 expression in tamoxifen resistance, we next examined the effect that combinatorial therapy with tamoxifen and trifluoperazine has on SGK1. For these experiments, ST88-14 cells were treated for 10 minutes to 24 hours with 2 μM tamoxifen and 5 μM trifluoperazine. Lysates of these cells were immunoblotted and probed with antibodies recognizing SGK1 or phosphorylated SGK1. Intriguingly, we found that the presence of trifluoperazine prevented the upregulation of SGK1 expression and phosphorylation that we observed in MPNST cells treated with tamoxifen alone (Fig. 7E); indeed, we observed no changes in SGK1 activity in the cells that underwent combined treatment when compared to vehicle control. These observations suggest that combinatorial therapy with tamoxifen and trifluoperazine may be more effective than monotherapy with either agent along because trifluoperazine targets distinct signaling cascades that impede the induction of molecules such as SGK1.

DISCUSSION

We have previously demonstrated that tamoxifen inhibits cultured MPNST cell survival and proliferation in an ER-independent manner and that this drug impedes the growth of orthotopic xenografts of MPNST cells. While encouraging, this study raised important new questions regarding the role that sex steroids play in MPNST pathogenesis in vivo, the maximal inhibitory effect tamoxifen could exert on MPNST growth, how the effectiveness of tamoxifen compared to that of trifluoperazine, whether combinatorial therapy with tamoxifen and trifluoperazine was more effective than either agent alone and, if so, whether this reflected differences in the signaling cascades targeted by these drugs. In keeping with our previous in vitro studies, our current findings argue that tamoxifen does not induce MPNST cell death in vivo via inhibition of sex steroid signaling, as no difference in tumor mass was observed in animals that underwent gonadectomy vs. sham controls. We have also demonstrated that tamoxifen or trifluoperazine monotherapy are similarly effective, decreasing xenograft size by 40% to 50%. In contrast, combinatorial treatment of grafted MPNST cells with tamoxifen and trifluoperazine decreased tumor weight via both cytostatic and cytotoxic effects compared to monotherapy or vehicle control; this dual treatment regimen was effective on both sporadic and NF1 associated MPNST cells and showed no

differences between the sexes. Finally, consistent with the effectiveness of combinatorial tamoxifen-trifluoperazine therapy, our kinomics analyses indicate that, while these 2 drugs target some of the same molecules, other proteins are uniquely affected by trifluoperazine, including a signaling cascade mediating tamoxifen resistance in other cancer types. Collectively, these findings provide guidance as to the most effective means of using tamoxifen and trifluoperazine to treat patients with MPNSTs. Our findings also raise intriguing questions regarding the role that the molecules implicated by our kinomics analyses play in MPNST biology and their potential utility as therapeutic targets.

It has long been recognized that the growth of NF1-associated dermal neurofibromas accelerates during puberty and pregnancy, which has led to the hypothesis that these tumors are hormonally sensitive. The evidence for a role of these hormones in MPNST pathogenesis is considerably more mixed (27). It has been reported that the growth of xenografts of sNF96.2 MPNST cells is enhanced by exogenous estrogen (18) and that ovariectomy diminishes the growth of grafts of these same cells (28). We previously demonstrated that surgically resected human MPNSTs and MPNST cell lines express estrogen receptor-β, G-protein coupled estrogen receptor-1 (GPER1), and the rate limiting biosynthetic enzymes in the 2 major estradiol biosynthetic pathways. However, we found no evidence that estradiol promoted the proliferation of these cells or rescued tamoxifen effects on MPNST cells. Instead, our findings indicated that tamoxifen affects MPNST survival and proliferation in an estrogen receptor-independent manner in vitro (6). Nonetheless, we were loath to rule out the possibility that signaling by estrogen or other gonadally derived hormones might promote MPNST growth in vivo via mechanisms such as interactions between estradiol and unknown cofactors present in the intratumoral microenvironment. Our demonstration that ovariectomy or castration had no effect on the growth of orthotopically xenografted human STS88-14 MPNST cells is consistent with our previous in vitro observations and argues that neither estrogen nor other gonadally derived circulating factors promote MPNST growth in vivo. It is unclear why our results differ from those presented in the earlier above noted studies. One possible explanation is that there are MPNST subtypes, only a small subset of which proliferative in response to estradiol; this would be consistent with our demonstration that MPNSTs routinely express ERβ and GPER1. It is also conceivable that the difference between our in vivo results and the previous study referenced above may to some extent reflect the physiology of the mouse strains used, since we used NSG mice for our orthotopic xenografts and Li et al used *Nf1*$^{+/-}$;*scid* mice for their studies (18). Nonetheless, the preponderance of our evidence indicates that neither estradiol nor other gonadally derived hormones promote the growth of the majority of MPNSTs.

In this study, we found that monotherapy with either tamoxifen or trifluoperazine produces a maximal 40% to 50% reduction in the mass of MPNST xenografts. Like many pharmacologic agents, the effects of tamoxifen and trifluoperazine are complex and these drugs affect multiple cytoplasmic targets. As the collection of proteins targeted by tamoxifen and trifluoperazine are only partially overlapping (see below), we hypothesized that combinatorial therapy with tamoxifen and trifluoperazine would additively or synergistically inhibit the growth of orthotopically xenografted MPNST cells. Upon testing this hypothesis in large cohorts of mice, we found that these drugs did indeed have additive effects on

MPNST growth, inhibiting the expansion of our xenografts to a much greater extent than could be achieved with tamoxifen or trifluoperazine alone. Interestingly, the responsiveness of MPNSTs to combinatorial therapy with tamoxifen and trifluoperazine does not appear to be dependent on the NF1 status of the tumor cells as we found that the NF1-associated ST88-14 line and the sporadic STS-26T line, which has been shown to have intact *NF1* alleles (29), showed similar decreases in tumor mass and proliferation and increased apoptosis in response to this treatment regimen. Of note, combinatorial therapy with tamoxifen and trifluoperazine has been shown to perform better than therapy with either agent alone in at least some other tumor types. For instance, trifluoperazine has synergistic effects with tamoxifen treatment in both ER positive and ER negative breast cancer cells (30). As tamoxifen and trifluoperazine are both currently in clinical use for other conditions (breast cancer and schizophrenia, respectively), our findings suggest that combinatorial therapy with tamoxifen and trifluoperazine could rapidly be adapted for clinical use in patients with MPNSTs.

Although our findings indicate that tamoxifen and trifluoperazine are effective against MPNSTs, the mechanisms by which these drugs act on MPNSTs and other tumor types are not completely understood. There is good reason to think that both agents act on multiple intracellular targets to exert their anti-tumorigenic effects. For example, in addition to its anti-estrogenic effects, tamoxifen inhibits calmodulin (31), protein kinase C (32, 33), and the MAPK pathway (34) in breast cancer, and selectively degrades K-Ras via autophagy in MPNST cells (7). We reasoned that globally examining tamoxifen and trifluoperazine effects on the kinome of MPNST cells would clarify the targets of these drugs, point to novel signaling cascades important for MPNST pathogenesis, and provide a mechanistic underpinning for combinatorial tamoxifen-trifluoperazine therapy. Upon performing our kinomic analyses, we found that these inhibitors did act on some of the same molecules. For instance, both tamoxifen and trifluoperazine targeted Akt, Erk1/2, and JNK signaling, which is consistent with our previous data (7); notably, Akt and Erk1/2 have been previously identified as key signaling molecules involved in MPNST pathogenesis.

Nonetheless, there were also some clear differences in the effects that tamoxifen and trifluoperazine exerted on the kinome of MPNST cells. Trifluoperazine targeted several kinases that were unaffected by tamoxifen, including PIM1 and PIM3. The PIM family of proto-oncogenes encodes several serine/threonine kinases that regulate cell cycle progression, apoptosis and transcription to promote tumorigenesis (35). For instance, phosphorylation of PIM1 or PIM3 can prevent Bad-mediated apoptosis in colon cancer (36) and pancreatic cancer (37). PIM1 phosphorylation has also been linked to the development of chemoresistance in hypoxic conditions via regulation of the mitochondrial transmembrane potential in pancreatic, cervical and colon cancer cells (38, 39). Inhibition of PIM kinases in prostate, breast and colon cancer decreases tumor cell proliferation while increasing apoptosis (40, 41). Interestingly, PIM kinases have not previously been implicated in MPNST pathogenesis. Consequently, it will be of interest to examine the function of these proteins in MPNSTs.

It was also notable that trifluoperazine inhibited the phosphorylation of SGK1 and SGK2. Although neither of these kinases has been previously implicated in MPNST pathogenesis,

they have been previously linked to tamoxifen resistance in other cancer types. Expression of SGK1 is elevated in tamoxifen-resistant breast tumors (25). Further, knocking down SGK1 renders drug-resistant breast cancer cells more sensitive to Akt inhibition (42). These observations in breast cancer make our finding that SGK1 expression is induced in MPNST cells challenged with tamoxifen and that co-administration of trifluoperazine prevents tamoxifen-induced SGK1 expression particularly striking. Considered together, these findings suggest that combinatorial tamoxifen-trifluoperazine therapy may be particularly effective against MPNSTs because trifluoperazine prevents MPNST cells from enabling the expression and phosphorylation of SGK1 in response to tamoxifen, an event that gives MPNST cells a measure of protection from tamoxifen. In future studies, it will be of interest to examine this possibility further with an eye towards manipulating SGK1 action in patients receiving tamoxifen therapy for MPNSTs.

In summary, tamoxifen and trifluoperazine both have profound effects on MPNST survival and proliferation in vivo. Because gonadectomy does not affect the growth of MPNST xenografts, these effects are likely estrogen receptor-independent. We have also shown that combinatorial treatment with tamoxifen and trifluoperazine is highly effective against MPNST orthotopic xenografts, regardless of whether the cells are derived from NF1-associated or sporadic MPNSTs. Our global kinomics analyses demonstrate that tamoxifen and trifluoperazine act on some of the same key signaling cascades in MPNSTs (e.g. Akt and Erk1/2). However, trifluoperazine also acts on several distinct signaling cascades, including PIM kinases and SGK1, which may contribute not only to cell death, but also to protection against tamoxifen treatment. Considered collectively, these findings suggest that tamoxifen and trifluoperazine may be useful for the treatment of patients suffering from MPNSTs. However, before these agents can advance to clinical trials in humans, it will be important to determine whether they are similarly effective against established MPNSTs arising in models such as mice that are genetically engineered to develop these neoplasms. It will also be of interest to determine whether NF1 patients (who are at high risk for the development of MPNSTs) will benefit from prophylactic treatment with tamoxifen, trifluoperazine, or both agents. While we do recognize that long-term treatment with tamoxifen or trifluoperazine carries its own risks, these drugs are given to some patient populations, including teens, for other chronic conditions. Given this, we should consider the possibility that the most effective way of dealing with MPNSTs in NF1 patients is to keep these patients from developing MPNSTs in the first place.

Supplementary Material

Refer to Web version on PubMed Central for supplementary material.

ACKNOWLEDGMENTS

We thank the Alabama Neuroscience Blueprint Core (P30 NS57098) and the UAB Neuroscience Core (P30 NS47466) for technical assistance. The content is solely the responsibility of the authors and does not necessarily represent the official views of the National Institutes of Health or the Department of Defense.

Supported by the National Institute of Neurological Diseases and Stroke (R01 NS048353 to S.L.C.; F31 NS081824 to S.N.B.), the National Cancer Institute (R01 CA122804 to S.L.C., R01 CA134773 to K.A.R.) and the Department of Defense (X81XWH-09-1-0086 and W81XWH-12-1-0164 to S.L.C.). The Genetically Defined Microbe and

Expression Core of the UAB Mucosal HIV and Immunology Center, which performed the lentiviral transduction of MPNST cells, was supported by R24 DK64400.

REFERENCES

1. Evans DG, Baser ME, McGaughran J, et al. Malignant peripheral nerve sheath tumours in neurofibromatosis 1. J Med Genet. 2002; 39:311–4. [PubMed: 12011145]
2. McCaughan JA, Holloway SM, Davidson R, et al. Further evidence of the increased risk for malignant peripheral nerve sheath tumour from a Scottish cohort of patients with neurofibromatosis type 1. J Med Genet. 2007; 44:463–6. [PubMed: 17327286]
3. Woodruff, JM.; Kourea, HP.; Louis, DN., et al. Malignant peripheral nerve sheath tumour (MPNST). In: Kleihues, PC.; Cavenee, WK., editors. Pathology and Genetics of Tumours of the Nervous System. IARC Press; Lyon: 2000. p. 172-4.
4. Ducatman BS, Scheithauer BW, Piepgras DG, et al. Malignant peripheral nerve sheath tumors. A clinicopathologic study of 120 cases. Cancer. 1986; 57:2006–21. [PubMed: 3082508]
5. Carroll SL, Ratner N. How does the Schwann cell lineage form tumors in NF1? Glia. 2008; 56:1590–605. [PubMed: 18803326]
6. Byer SJ, Eckert JM, Brossier NM, et al. Tamoxifen inhibits malignant peripheral nerve sheath tumor growth in an estrogen receptor-independent manner. Neuro-oncology. 2011; 13:28–41. [PubMed: 21075781]
7. Kohli L, Kaza N, Coric T, et al. 4-Hydroxytamoxifen induces autophagic death through K-Ras degradation. Cancer Res. 2013; 73:4395–405. [PubMed: 23722551]
8. Stonecypher MS, Byer SJ, Grizzle WE, et al. Activation of the neuregulin-1/ErbB signaling pathway promotes the proliferation of neoplastic Schwann cells in human malignant peripheral nerve sheath tumors. Oncogene. 2005; 24:5589–605. [PubMed: 15897877]
9. Eckert JM, Byer SJ, Clodfelder-Miller BJ, et al. Neuregulin-1 beta and neuregulin-1 alpha differentially affect the migration and invasion of malignant peripheral nerve sheath tumor cells. Glia. 2009; 57:1501–20. [PubMed: 19306381]
10. Rivera A, Rivera E, Giono S, et al. Cell cultures contaminations by mycoplasmas. African Journal of Microbiology Research. 2009; 3:637–40.
11. Nagy A, Gertsenstein M, Vintersten K, et al. CSH Protoc. 2006; 2006
12. Strom JO, Theodorsson A, Ingberg E, et al. Ovariectomy and 17beta-estradiol replacement in rats and mice: a visual demonstration. J Vis Exp. 2012:e4013. [PubMed: 22710371]
13. McAsey ME, Cady C, Jackson LM, et al. Time course of response to estradiol replacement in ovariectomized mice: brain apolipoprotein E and synaptophysin transiently increase and glial fibrillary acidic protein is suppressed. Exp Neurol. 2006; 197:197–205. [PubMed: 16226751]
14. Wichmann MW, Zellweger R, DeMaso CM, et al. Mechanism of immunosuppression in males following trauma-hemorrhage. Critical role of testosterone. Arch Surg. 1996; 131:1186–91. discussion 91-2. [PubMed: 8911259]
15. Turk AN, Byer SJ, Zinn KR, et al. Orthotopic xenografting of human luciferase-tagged malignant peripheral nerve sheath tumor cells for in vivo testing of candidate therapeutic agents. J Vis Exp. 2011; 49:e2558.
16. Carroll SL, Miller ML, Frohnert PW, et al. Expression of neuregulins and their putative receptors, ErbB2 and ErbB3, is induced during Wallerian degeneration. J Neurosci. 1997; 17:1642–59. [PubMed: 9030624]
17. Carroll SL. Molecular mechanisms promoting the pathogenesis of Schwann cell neoplasms. Acta Neuropathol. 2012; 123:321–48. [PubMed: 22160322]
18. Li H, Zhang X, Fishbein L, et al. Analysis of steroid hormone effects on xenografted human NF1 tumor schwann cells. Cancer Biol Ther. 2010; 10:758–64. [PubMed: 20699653]
19. Lam HY. Tamoxifen is a calmodulin antagonist in the activation of cAMP phosphodiesterase. Biochem Biophys Res Commun. 1984; 118:27–32. [PubMed: 6320825]
20. Vandonselaar M, Hickie RA, Quail JW, et al. Trifluoperazine-induced conformational change in Ca(2+)-calmodulin. Nat Struct Biol. 1994; 1:795–801. [PubMed: 7634090]

21. Mandlekar S, Kong AN. Mechanisms of tamoxifen-induced apoptosis. Apoptosis. 2001; 6:469–77. [PubMed: 11595837]
22. Hayashi M, Tapping RI, Chao TH, et al. BMK1 mediates growth factor-induced cell proliferation through direct cellular activation of serum and glucocorticoid-inducible kinase. J Biol Chem. 2001; 276:8631–4. [PubMed: 11254654]
23. Mikosz CA, Brickley DR, Sharkey MS, et al. Glucocorticoid receptor-mediated protection from apoptosis is associated with induction of the serine/threonine survival kinase gene, sgk-1. J Biol Chem. 2001; 276:16649–54. [PubMed: 11278764]
24. Brunet A, Park J, Tran H, et al. Protein kinase SGK mediates survival signals by phosphorylating the forkhead transcription factor FKHRL1 (FOXO3a). Mol Cell Biol. 2001; 21:952–65. [PubMed: 11154281]
25. Sommer EM, Dry H, Cross D, et al. Elevated SGK1 predicts resistance of breast cancer cells to Akt inhibitors. Biochem J. 2013; 452:499–508. [PubMed: 23581296]
26. Webster MK, Goya L, Ge Y, et al. Characterization of sgk, a novel member of the serine/threonine protein kinase gene family which is transcriptionally induced by glucocorticoids and serum. Mol Cell Biol. 1993; 13:2031–40. [PubMed: 8455596]
27. Fishbein L, Zhang X, Fisher LB, et al. In vitro studies of steroid hormones in neurofibromatosis 1 tumors and Schwann cells. Mol Carcinog. 2007; 46:512–23. [PubMed: 17393410]
28. Perrin GQ, Li H, Fishbein L, et al. An orthotopic xenograft model of intraneural NF1 MPNST suggests a potential association between steroid hormones and tumor cell proliferation. Lab Invest. 2007; 87:1092–102. [PubMed: 17876295]
29. Miller SJ, Rangwala F, Williams J, et al. Large-scale molecular comparison of human schwann cells to malignant peripheral nerve sheath tumor cell lines and tissues. Cancer Res. 2006; 66:2584–91. [PubMed: 16510576]
30. Frankfurt OS, Sugarbaker EV, Robb JA, et al. Synergistic induction of apoptosis in breast cancer cells by tamoxifen and calmodulin inhibitors. Cancer Lett. 1995; 97:149–54. [PubMed: 7497456]
31. O'Brian CA, Ioannides CG, Ward NE, et al. Inhibition of protein kinase C and calmodulin by the geometric isomers cis- and trans-tamoxifen. Biopolymers. 1990; 29:97–104. [PubMed: 2158363]
32. Gundimeda U, Chen ZH, Gopalakrishna R. Tamoxifen modulates protein kinase C via oxidative stress in estrogen receptor-negative breast cancer cells. J Biol Chem. 1996; 271:13504–14. [PubMed: 8662863]
33. Cabot MC, Zhang Z, Cao H, et al. Tamoxifen activates cellular phospholipase C and D and elicits protein kinase C translocation. Int J Cancer. 1997; 70:567–74. [PubMed: 9052757]
34. Mandlekar S, Yu R, Tan TH, et al. Activation of caspase-3 and c-Jun NH2-terminal kinase-1 signaling pathways in tamoxifen-induced apoptosis of human breast cancer cells. Cancer Res. 2000; 60:5995–6000. [PubMed: 11085519]
35. Bachmann M, Moroy T. The serine/threonine kinase Pim-1. Int J Biochem Cell Biol. 2005; 37:726–30. [PubMed: 15694833]
36. Popivanova BK, Li YY, Zheng H, et al. Proto-oncogene, Pim-3 with serine/threonine kinase activity, is aberrantly expressed in human colon cancer cells and can prevent Bad-mediated apoptosis. Cancer Sci. 2007; 98:321–8. [PubMed: 17270021]
37. Li YY, Popivanova BK, Nagai Y, et al. Pim-3, a proto-oncogene with serine/threonine kinase activity, is aberrantly expressed in human pancreatic cancer and phosphorylates bad to block bad-mediated apoptosis in human pancreatic cancer cell lines. Cancer Res. 2006; 66:6741–7. [PubMed: 16818649]
38. Chen J, Kobayashi M, Darmanin S, et al. Hypoxia-mediated up-regulation of Pim-1 contributes to solid tumor formation. Am J Pathol. 2009; 175:400–11. [PubMed: 19528349]
39. Chen J, Kobayashi M, Darmanin S, et al. Pim-1 plays a pivotal role in hypoxia-induced chemoresistance. Oncogene. 2009; 28:2581–92. [PubMed: 19483729]
40. Hu XF, Li J, Vandervalk S, et al. PIM-1-specific mAb suppresses human and mouse tumor growth by decreasing PIM-1 levels, reducing Akt phosphorylation, and activating apoptosis. J Clin Invest. 2009; 119:362–75. [PubMed: 19147983]
41. Weirauch U, Beckmann N, Thomas M, et al. Functional role and therapeutic potential of the pim-1 kinase in colon carcinoma. Neoplasia. 2013; 15:783–94. [PubMed: 23814490]

42. Moniz LS, Vanhaesebroeck B. AKT-ing out: SGK kinases come to the fore. Biochem J. 2013; 452:e11–3. [PubMed: 23725458]

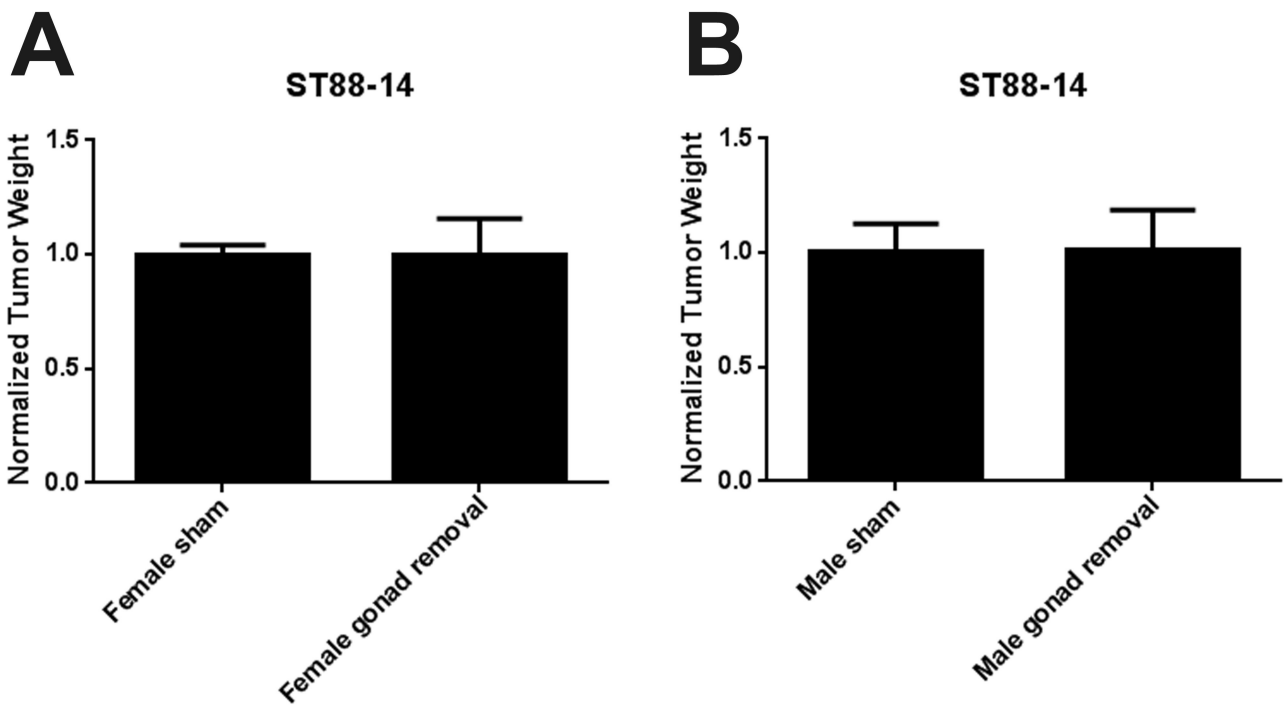

Figure 1.

Gonadally derived sex hormones do not influence the growth of orthotopically xenografted malignant peripheral nerve sheath tumor (MPNST) cells. (**A**) Comparison of grafts weights (indicated as mean with SE) in sham or ovariectomized mice. (**B**) Comparison of grafts weights (indicated as mean with SE) in sham or ovariectomized mice.

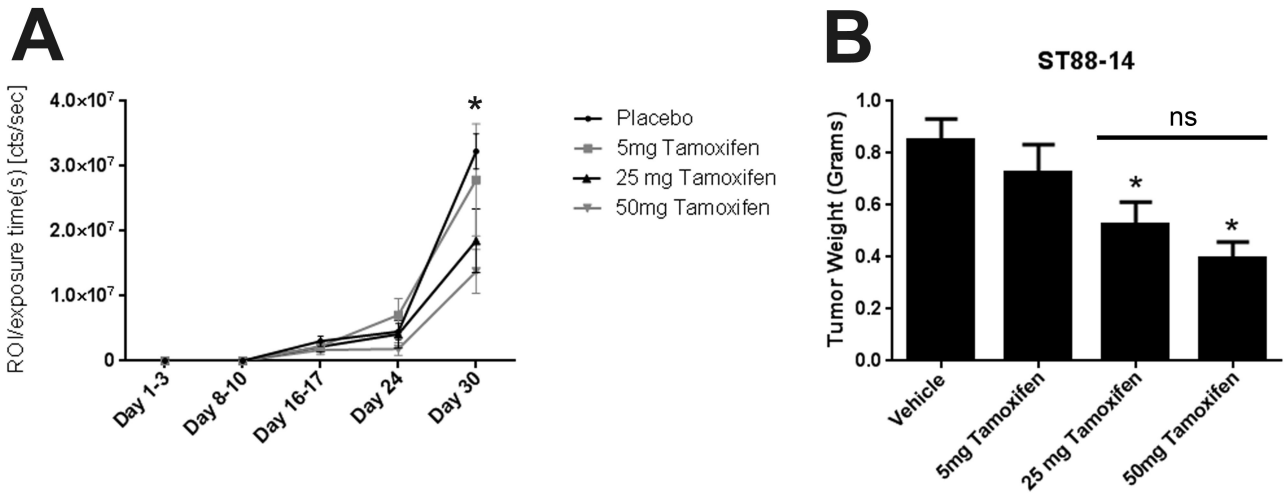

Figure 2.

(**A**) Bioluminescent signals from malignant peripheral nerve sheath tumor (MPNST) grafts 1-30 d post-grafting in animals treated with placebo pellets (vehicle) or pellets containing 5, 25 or 50 mg of tamoxifen. *$p < 0.05$ vs. placebo. (**B**) MPNST graft weights from mice treated with placebo or pellets containing 5, 25 or 50 mg tamoxifen. *$p < 0.05$ vs. vehicle. The bar with ns (non-significant) is for comparison of grafts from mice receiving 25 or 50 mg tamoxifen.

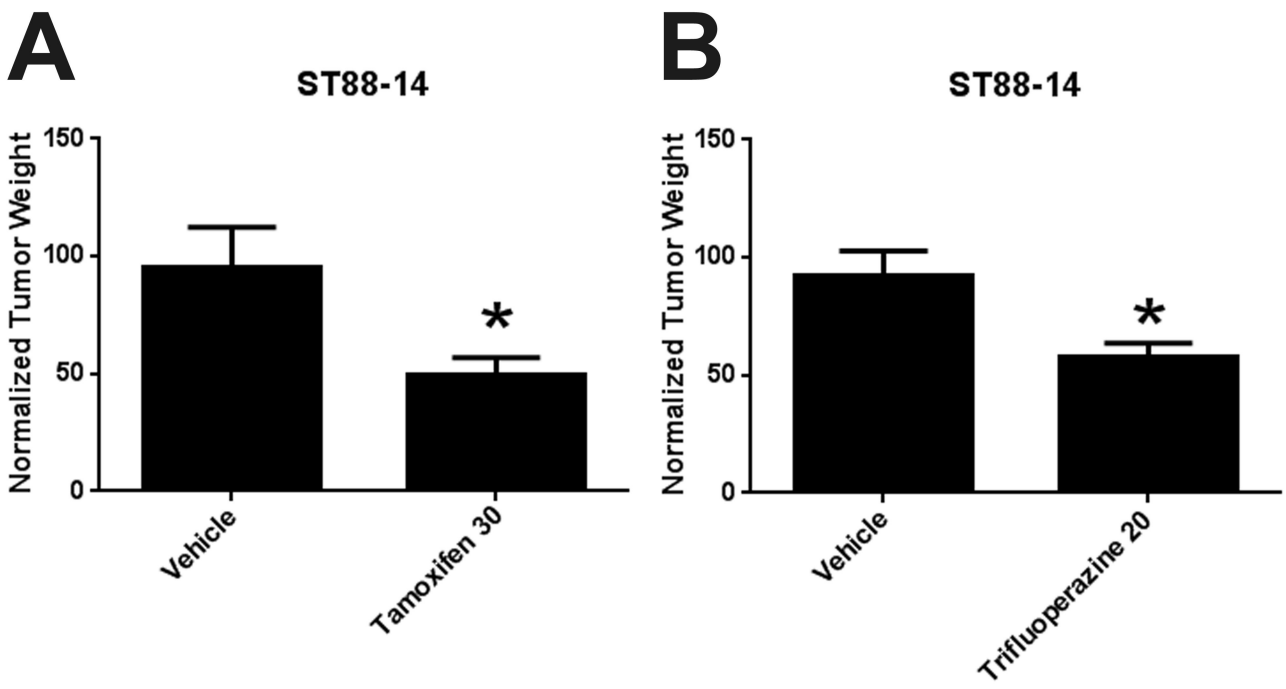

Figure 3.

(**A, B**) Xenograft weight was reduced by 50% with tamoxifen (**A**) or 40% with trifluoperazine (**B**) administered via intraperitoneal injection. Both drugs were administered at their maximally tolerated dose. *$p < 0.05$.

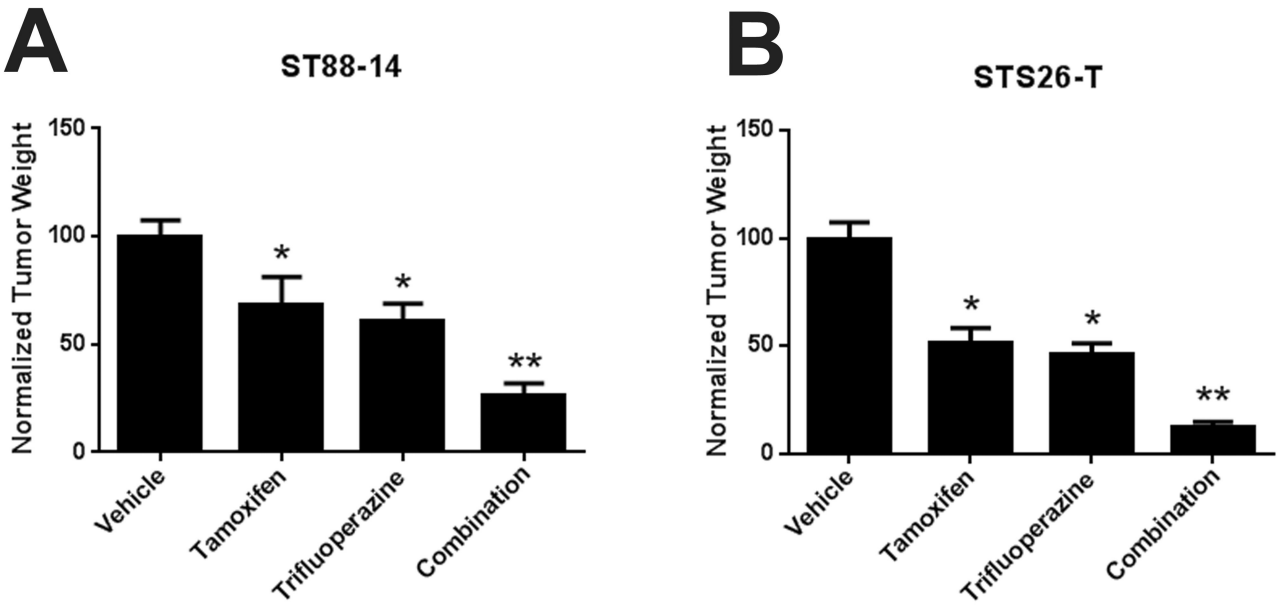

Figure 4.

(**A**) Combinatorial treatment with tamoxifen and trifluoperazine causes further decreases in xenograft mass in NF1-associated (ST88-14) malignant peripheral nerve sheath tumor (MPNST) cells. (**B**) Combinatorial treatment with tamoxifen and trifluoperazine also enhances decreases in xenograft mass in mice grafted with sporadic STS-26T MPNST cells. *$p < 0.05$ vs. vehicle control; **$p < 0.05$ vs. either tamoxifen- or trifluoperazine-treated animals.

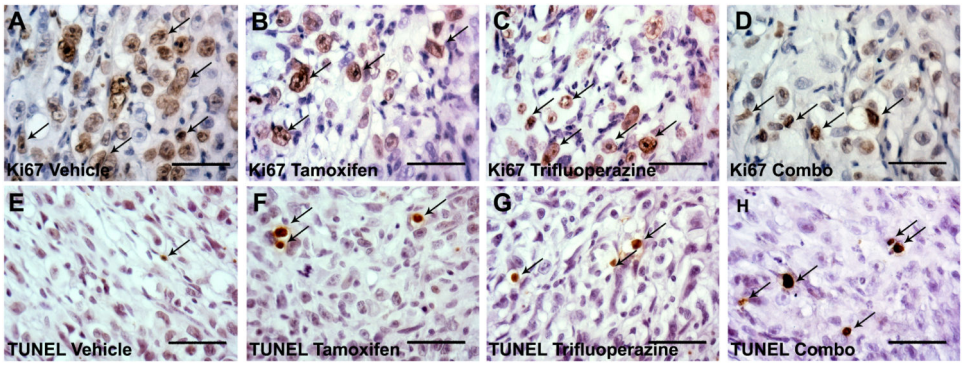

Figure 5.

(**A-D**) When compared to vehicle control (**A**), treatment with tamoxifen (**B**), trifluoperazine (**C**), or a combination (Combo) of the 2 agents (**D**) results in decreased Ki67 staining. (**E-H**) Increased levels of apoptosis, as determined by terminal deoxynucleotidyl transferase dUTP nick end labeling (TUNEL), were observed when comparing vehicle (**E**), tamoxifen- (**F**), trifluoperazine- (**G**), or dual-treated (**H**) xenografted ST88-14 cells. Arrows indicate representative positive cells for Ki67 or TUNEL labeling.

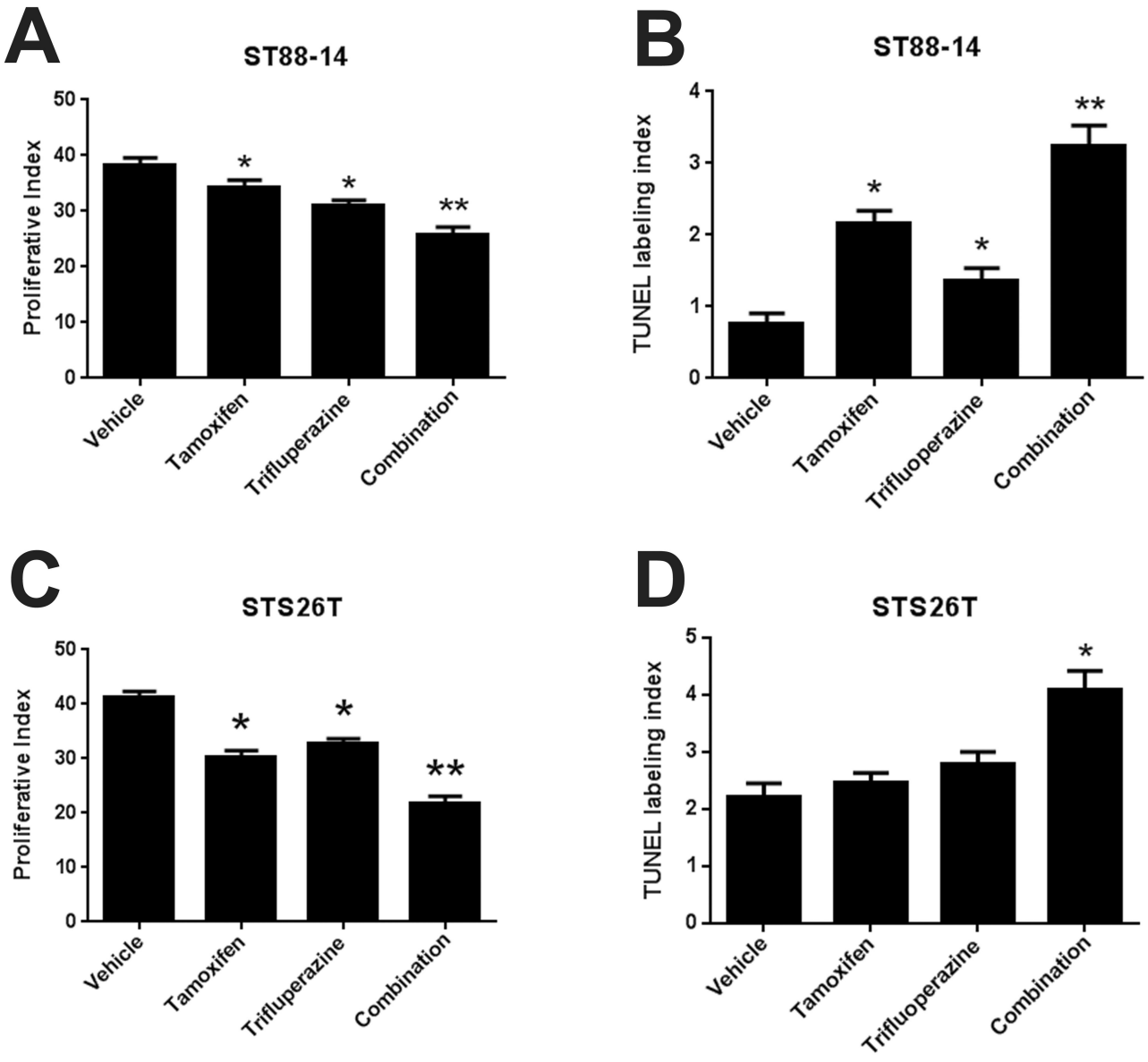

Figure 6.

(**A**-**D**) In both ST88-14 (**A, B**) and STS-26T (**C, D**) cells, combinatorial treatment with tamoxifen and trifluoperazine decreases cellular proliferation (**A, C**) and increases apoptosis (**B, D**) to a greater extent than is seen with monotherapy with either agent alone. *$p < 0.05$ vs. vehicle control; **$p < 0.05$ vs. either tamoxifen- or trifluoperazine-treated animals.

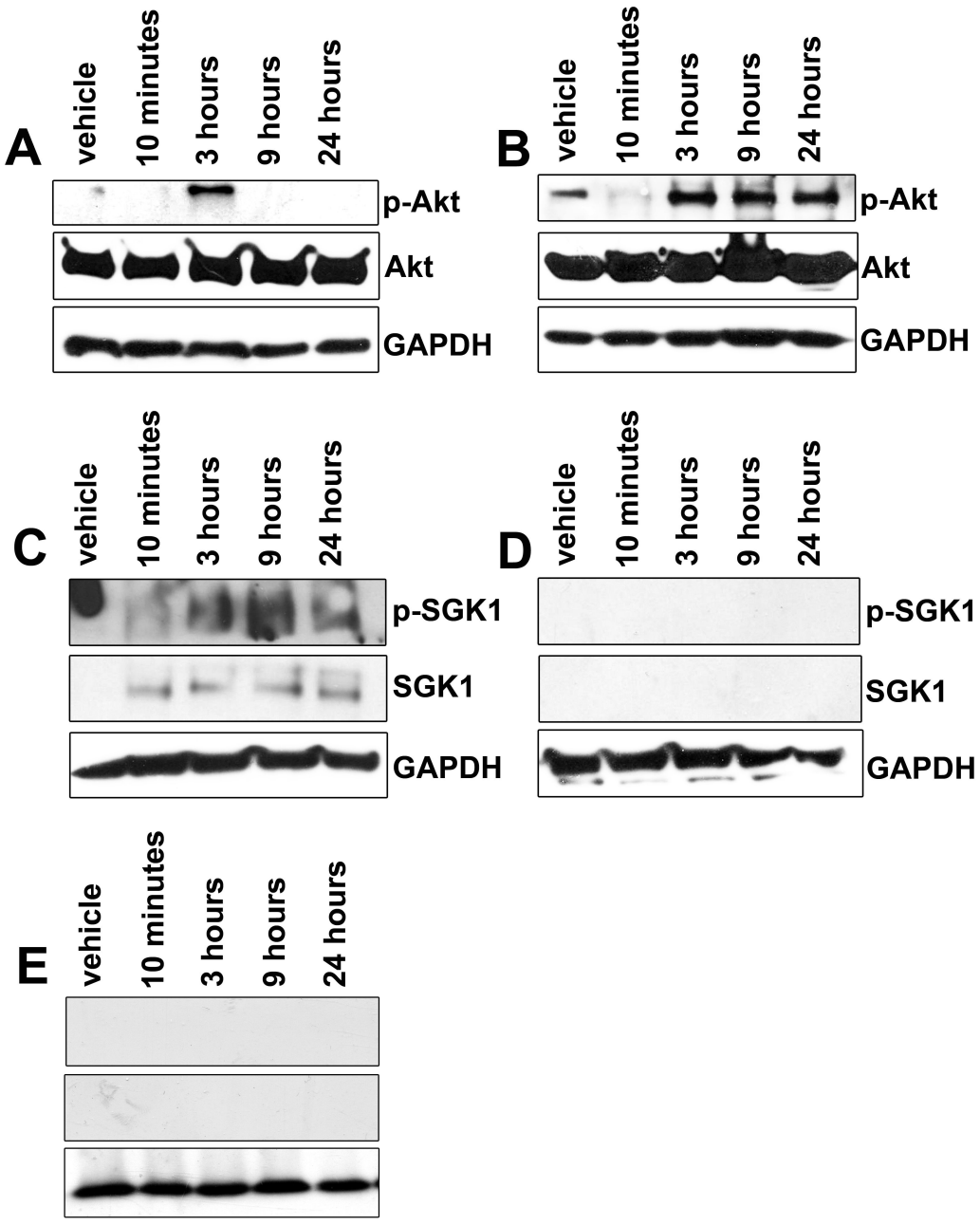

Figure 7.

(**A, B**) Western blots demonstrating decreased Akt signaling at 10 minutes in both tamoxifen- (**A**) and trifluoperazine (**B**)-treated ST88-14 cells; a transient recovery of p-Akt is seen at 3 hours only in tamoxifen-treated cells, whereas it more robustly recovers in trifluoperazine- treated cells. (**C, D**) Tamoxifen treatment also increases the expression and phosphorylation of SGK1 (**C**). In contrast, SGK1 expression is not observed in trifluoperazine-treated cells (**D**). (**E**) When administered in combination with tamoxifen, trifluoperazine treatment is sufficient to prevent the tamoxifen-mediated increase in SGK1

expression and phosphorylation seen when cultured ST88-14 cells are treated with tamoxifen alone. GAPDH, glyceraldehyde 3-phosphate dehydrogenase.

Table

Kinase Signaling Decreased by Trifluoperazine Relative to Tamoxifen Treatment*

Kinase Inhibited by Trifluoperazine Treatment	Score
Pim3	6556.9904
PKACα	10936.7912
Akt1	1326.054
Erk1	1730.7
p70 S6 kinase b	13791.8717
PKACβ	10872.7505
Akt2	11940.6309
Jnk1	1547.6943
Jnk3	1547.6943
Erk2	1586.3
PIM1	3845.0034
Akt3	15216.9059
PRKX	10364.6347
SGK1	10187.8735
CDK2	1270.45
SGK2	10183.8187

*Scores generated with the algorithms indicated in the Materials and Methods denote the likelihood that the indicated kinase is differentially affected. All of these kinases